This article has been accepted for publication in a future issue of this journal, but has not been fully edited. Content may change prior to final publication. Citation information: DOI 10.1109/LCOMM.2015.2423676, IEEE Communications Letters

Time-Domain Oversampled OFDM Communication in Doubly-Selective Underwater Acoustic Channels

Bo Peng, Pierluigi Salvo Rossi, *Senior Member, IEEE*,
Hefeng Dong, *Member, IEEE*, and Kimmo Kansanen, *Member, IEEE*

***Abstract*—This paper investigates the time-domain oversampled cyclic-prefix orthogonal frequency division multiplexing (CP-OFDM) system for communication over doubly-selective underwater acoustic channels. Channel estimation is based on two different time-varying channel models. One is the basis expansion model (BEM), the other is the Doppler-rate model (DRM). Exploiting the sparsity of underwater acoustic channels, orthogonal matching pursuit (OMP) is employed to obtain the time-varying channel state information (CSI). The receiver operates without any prior knowledge of the statistics of the CSI, as this information usually is unavailable for underwater acoustic channels. Channel estimation error and bit error rate (BER) performance of the system are demonstrated through numerical simulations. Results show that the oversampled CP-OFDM achieves significant gains over the conventional symbol-rate sampled system.**

***Index Terms*—Channel estimation, orthogonal frequency division multiplexing (OFDM), oversampling, underwater acoustic communication**

I. Introduction

UNDERWATER acoustic channels, usually characterized as doubly-selective (time and frequency selective) channels, are extremely challenging [1]. Orthogonal frequency division multiplexing (OFDM) has been widely investigated in order to implement reliable high data rate communication in underwater channels [1]–[5].

Conventionally, symbol-rate sampling is employed at the receiver and very limited works can be found on fractional sampling for OFDM systems, as opposed to single carrier systems [6]. Recently, the work in [7] showed that time-domain oversampling of OFDM can achieve potential multipath diversity in quasi-static fading channels. In [5], time-domain oversampling is employed on multi-input multi-output communications in quasi-static underwater acoustic channels. The work in [8] extended time-domain oversampling for OFDM system in doubly-selective channels, showing that both Doppler diversity and multipath diversity can be obtained. However, the result was based on the assumption that perfect time-varying channel state information (CSI) is available.

This paper investigates time-domain oversampling in OFDM communication systems for time-varying underwater acoustic channels, without the assumption that perfect CSI is available. Two different time-varying models are considered for channel estimation at receiver: one is the basis expansion model (BEM) [9]–[11], the other is Doppler-rate model (DRM) [2]. Additionally, we adopt orthogonal matching pursuit (OMP) [2], [12] to explore the sparsity of the underwater acoustic channels i.e. the most channel energy is concentrated on a few time delay and/or Doppler spread values. Linear minimum mean square error (LMMSE) equalization is implemented for data-symbol recovery and signal-to-noise ratio (SNR) is also estimated at receiver location. Bit error rate (BER) performance of the proposed time-domain oversampled receiver is evaluated through numerical simulations with appealing results in comparison to the conventional symbol-rate sampled receiver. The main contribution of the letter is to propose a practical receiver for underwater communications which is able to exploit time-domain oversampling and channel sparsity.

The rest of paper is organized as follows. The system model is presented in Section II. Section III describes the channel estimator and the equalizer. Section IV presents the simulation results and Section V provides some concluding remarks.

Notation: Upper-case (resp. lower-case) bold letters represent matrices (resp. column vectors) with $[A]_{n,m}$ (resp. a_n) denoting the (n, m)th (resp. nth) entry of $\mathbf{A}$ (resp. $\mathbf{a}$); $\mathtt{E}(\cdot)$, $(\cdot)^T$ and $(\cdot)^H$ denote expectation, transpose and Hermitian transpose operators, respectively, $\otimes$ is the Kronecker product, $\delta(t)$ denotes the Dirac delta function; $\mathbf{F}$ represents normalized Fourier matrix and $\tilde{\mathbf{a}} = \mathbf{F}\mathbf{a}$ denotes the FFT of $\mathbf{a}$; diag$(\mathbf{a})$ denotes a diagonal matrix with $\mathbf{a}$ on the main diagonal; $(\mathbf{a})_{\mathcal{P}}$ denotes a column vector with entries of $\mathbf{a}$ corresponding to the indices from the set $\mathcal{P}$; $\mathbf{1}_p$ is a $p \times 1$ column vector with all the elements being 1 and $\mathbf{I}$ denotes the identity matrix; $\hat{a}$ denotes the estimate of a.

II. System Model

A block of data with N symbols, $\mathbf{s} = [s_0, \cdots, s_{N-1}]^T$, are modulated on N subcarriers, generating N time-domain symbols as $v[n] = \frac{1}{\sqrt{N}} \sum_{k=0}^{N-1} s_k e^{\frac{j2\pi kn}{N}}$. To avoid inter-block interference, a cyclic prefix (CP) with length of N_{cp} is inserted in the beginning of each data block. After CP insertion, the time domain symbols are passed through a pulse shaping filter and modulated to the carrier frequency f_c. The baseband transmitted signal is $\sum_{n=-N_{cp}}^{N-1} v[n]p(t - nT_s)$, where $p(t)$ is the pulse shaping filter and T_s represents the symbol time.

This work was supported in part by the SensIs project funded by the Research Council of Norway (Grant No. 217234), and in part by the Faculty of Information Technology, Mathematics and Electrical Engineering, Norwegian University of Science and Technology, Trondheim, Norway, through the CAMOS Project.

The authors are with the Department of Electronics and Telecommunications, Norwegian University of Science and Technology, Trondheim 7491, Norway (e-mail: bo.peng@iet.ntnu.no; salvorossi@iet.ntnu.no; hefeng.dong@iet.ntnu.no; kimmo.kansanen@iet.ntnu.no)

A. BEM-Based Time-Domain Oversampled Signal Model

At receiver side, the received signal is first downconverted and sampled with the period $T = T_s/G$. The case $G = 1$ corresponds to the conventional OFDM receiver, while $G > 1$ represents oversampling. Therefore, the discrete-time model for the received signal can be written as

$$y_n = \sum_{l=0}^{L-1} h[n,l]x_{n-l} + w_n \tag{1}$$

where $h[n,l]$ is the discrete-time time-varying channel impulse response (CIR) with T spacing, $w[n]$ is the zero-mean white Gaussian noise with variance σ^2, and x_n is defined as

$$x_n = \begin{cases} s[\frac{n}{G}] & \text{if } \frac{n}{G} \text{ is integer} \\ 0 & \text{else} \end{cases}. \tag{2}$$

The time-varying channel tap with fixed delay at l is modelled by $Q-$order BEM as

$$h[n,l] = \sum_{q=0}^{Q-1} b_{q,l} v_n[q], \tag{3}$$

where $v_n[q]$ is the qth order base function and $b_{q,l}$ is the corresponding model coefficient. After CP removal, by replacing (3) into (1), we get

$$\mathbf{y} = \sum_{q=0}^{Q-1} \text{diag}(\mathbf{v}[q])\mathbf{B}[q]\mathbf{x} + \mathbf{w} \tag{4}$$

where $\mathbf{B}[q]$ is a circulant matrix whose first column is $[b_{q,0},\, b_{q,1},\, \cdots\, b_{q,L-1},\, 0,\, \cdots\, 0]^T$. Applying FFT on (4), we have

$$\tilde{\mathbf{y}} = \sum_{q=0}^{Q-1} \mathbf{\Delta}[q]\mathbf{F}\mathbf{B}[q]\mathbf{F}^H\underline{\mathbf{s}} + \tilde{\mathbf{w}} \tag{5}$$

where $\mathbf{\Delta}[q] = \mathbf{F}\text{diag}(\mathbf{v}[q])\mathbf{F}^H$ is a circulant matrix and $\underline{\mathbf{s}} = \mathbf{1}_G \otimes \mathbf{s}$ is an expanded vector taking into account oversampling. In our work, we use the discrete prolate spheroidal BEM (DPS-BEM) since the DPS-BEM does not require any prior information about channel statistics and can avoid the spectral leakage and Gibbs phenomenon in complex exponential BEM [10], [11]. Moreover, the method also works with other BEMs.

B. DRM-Based Time-Domain Oversampled Signal Model

DRM assumes the underwater acoustic channel is composed of distinguish paths with time-variant delays and time-invariant path gains. Therefore, the continuous-time CIR (excluding the pulse shaping filter) is modelled as in [2]

$$c(t,\tau) = \sum_{p=0}^{L_p-1} A_p \delta(\tau - \tau_p + a_p t), \tag{6}$$

where L_p is the number of paths and A_p, τ_p and a_p denote gain, delay and Doppler rate of the pth path, respectively. $C(t,f)$ denotes the corresponding time-variant transfer function. Therefore, the received signal, after CP removal, down-conversion and carrier frequency offset (CFO) compensation, can be written as

$$\begin{aligned} y(t) &= \int_{f_c-\frac{GB}{2}}^{f_c+\frac{GB}{2}} C(t,f)e^{j2\pi ft}U(f-f_c)e^{-j2\pi(f_c+\epsilon)t}df + w(t) \\ &= \sum_{p=0}^{L_p-1} \int_{-\frac{GB}{2}}^{\frac{GB}{2}} A_p U(f) e^{j2\pi[(f-\epsilon)t-(f_c+f)(\tau_p-a_p t)]}df + w(t) \end{aligned} \tag{7}$$

where ϵ denotes the CFO, $B = 1/T_s$ and $U(f) = V(f)P(f)$. $V(f)$ is the discrete time Fourier transform of $v[n]$ and $P(f)$ denotes the continuous frequency spectrum of the pulse shaping filter. In practice, $P(f)$ would be dependent on the power amplifier, transducer, and ocean propagation environment, therefore, we assume $P(f) = 1,\ f \in [-\frac{GB}{2}\ \frac{GB}{2}]$ in this paper for ease of computation. Performing CP-OFDM demodulation, we have

$$\begin{aligned} \tilde{y}_m &= \int_0^{T_b} y(t)e^{-j2\pi\frac{m}{T_b}t}\,dt \\ &= \sum_{p=0}^{L_p-1} \sum_{k=-\frac{GN}{2}}^{\frac{GN}{2}} A_p \gamma_p[k]\underline{s}_k \Gamma_p[m,k]\beta_p[m,k] + \tilde{w}_m \end{aligned} \tag{8}$$

where

$$\Gamma_p[m,k] = \text{sinc}\left(\pi\left(f_k(1+a_p) - f_m - \epsilon\right)T_b\right), \tag{9}$$

$$\beta_p[m,k] = e^{-j\pi(f_k(1+a_p)-f_m-\epsilon)T_b}, \tag{10}$$

$$\gamma_p[k] = e^{-j2\pi f_k \tau_p}. \tag{11}$$

Also, $f_k = f_c + \frac{k}{T_b}$ with $k = -\frac{GN}{2} \cdots \frac{GN}{2}$. The integration in (8) is realized by FFT in practical implementation.

III. Channel Estimation and Equalization

A. Channel Estimation

For channel estimation, we can represent both Eqs (5) and (8) in the form $\underline{\mathbf{y}} = \mathbf{U}\boldsymbol{\xi} + \underline{\boldsymbol{\omega}}$ where $\underline{\mathbf{y}}$ denotes the received signals at pilot subcarriers, $\boldsymbol{\xi}$ collects the unknown model parameters and $\mathbf{U}$ is a known model-dependent matrix.

More specifically, for BEM based model, it is straightforward to get $\boldsymbol{\xi} = \left[b_{0,0} \cdots b_{Q-1,L-1}\right]^T$ and $\mathbf{U} = \left[(\mathbf{\Delta}[0]\text{diag}(\mathbf{F}_1)\underline{\mathbf{s}})_{\mathcal{P}}, \cdots, (\mathbf{\Delta}[Q-1]\text{diag}(\mathbf{f}_L)\underline{\mathbf{s}})_{\mathcal{P}}\right]$, where $\mathbf{F}_l$ is the lth column of matrix $\mathbf{F}$.

For the DRM based receiver, we follow the method in [2] to construct $\mathbf{U}$ and $\boldsymbol{\xi}$. We define the overparameterized 2-D dictionary $\{a,\, \tau\}$ over an $N_a \times N_\tau$ grid as

$$a \in \{-a_{max},\, -a_{max} + \Delta a,\, \cdots,\, a_{max}\}, \tag{12}$$

$$\tau \in \{0,\, \frac{T_b}{\lambda N},\, \cdots,\, \tau_{max}\}, \tag{13}$$

where Δa and $T_b/\lambda N$ represent steps along delay axis and Doppler-rate axis respectively, then $\boldsymbol{\xi} = \left[A_{1,1} \cdots A_{N_a,N_\tau}\right]^T$ and

$$\mathbf{U} = \left[(\mathbf{\Phi}[1]\mathbf{\Xi}[1]\underline{\mathbf{s}})_{\mathcal{P}},\, \cdots,\, (\mathbf{\Phi}[N_a]\mathbf{\Xi}[N_\tau]\underline{\mathbf{s}})_{\mathcal{P}}\right]. \tag{14}$$

Matrix $\mathbf{\Phi}[p]$ has entries as

$$\left[\Phi[p]\right]_{m,k} = \Gamma_p[m,k]\beta_p[m,k], \tag{15}$$

This article has been accepted for publication in a future issue of this journal, but has not been fully edited. Content may change prior to final publication. Citation information: DOI 10.1109/LCOMM.2015.2423676, IEEE Communications Letters

and $\boldsymbol{\Xi}[p] = \mathrm{diag}(\gamma_p[1], \cdots, \gamma_p[N_\tau])$.

Since the underwater acoustic channel often exhibits sparsity, we can use compressed sensing technique to explore the channel sparsity. In this paper, the OMP algorithm [12] is employed. The OMP searching process stops when a predefined iteration number M is reached. For the DPS-BEM model, the channel sparsity often exists only in the delay domain. Therefore, we use the 1-D search for the DPS-BEM model and the searching criteria in the sth iteration of the OMP algorithm is modified as

$$i = \arg\max_{i \in E_s} \sum_{j=(i-1)Q+1}^{iQ} \frac{\|\mathbf{U}_j^H \underline{\mathbf{y}}^{(s)}\|}{\|\mathbf{U}_j\|}, \tag{16}$$

where $\mathbf{U}_j$ is the jth column of matrix $\mathbf{U}$, $\underline{\mathbf{y}}^{(s)}$ is the remaining vector after $(s-1)$th iteration and E_s represents the searching subset in the sth iteration.

Once the estimation of $\boldsymbol{\xi}$ is performed, we can construct the estimate of channel matrix as

$$\hat{\mathbf{H}} = \sum_{q=0}^{Q-1} \sum_{l=1}^{L} \hat{b}_{q,l} \boldsymbol{\Delta}_q \mathrm{diag}(\mathbf{f}_l) \tag{17}$$

for the DPS-BEM-based receiver, and

$$\hat{\mathbf{H}} = \sum_{i=1}^{N_a} \sum_{j=1}^{N_\tau} \hat{A}_{i,j} \boldsymbol{\Phi}[i] \boldsymbol{\Xi}[j] \tag{18}$$

for the DRM-based receiver.

B. Equalizer

With the estimated channel matrix $\hat{\mathbf{H}}$, the received signal can be written as

$$\tilde{\mathbf{y}} = \hat{\mathbf{H}} \underline{\mathbf{s}} + \boldsymbol{\omega}, \tag{19}$$

where $\boldsymbol{\omega}$ is the equivalent noise including the system noise, ICI and the model error. Eq. (19) can be further written as

$$\tilde{\mathbf{y}} = \underline{\hat{\mathbf{H}}} \mathbf{s} + \boldsymbol{\omega}, \tag{20}$$

where $\underline{\hat{\mathbf{H}}} = \hat{\mathbf{H}} \mathbf{I}_\mathbf{G}$ and $\mathbf{I}_\mathbf{G} = \mathbf{1}_\mathbf{G} \otimes \mathbf{I}$, from which it is apparent that the oversampled system could be regarded as a single-input multiple-output communication system. We use LMMSE equalizer to obtain the symbol estimation as

$$\hat{\mathbf{s}} = \left(\underline{\hat{\mathbf{H}}}^H \underline{\hat{\mathbf{H}}} + \sigma_0^2 \mathbf{I} \right)^{-1} \underline{\hat{\mathbf{H}}}^H \tilde{\mathbf{y}} \tag{21}$$

where σ_0^2 is the variance of the equivalent noise ($\boldsymbol{\omega}$) which is approximated white Gaussian, and is estimated by averaging the signal power in the null sub-carriers as in [4].

IV. Simulation Results

Numerical simulations refer to a six-path channel with path amplitudes drawn from Rayleigh distribution. Path gains decrease exponentially with the difference between the first path and the last path being 6 dB. Path delays are randomly distributed with maximum delay spread equal to 25 ms and the minimum time difference between two paths being 0.25 ms. Doppler-rate coefficients are drawn from zero-mean uniform distribution with standard velocity deviation $\delta_v = 0.05m/s$, i.e. the ratio between the maximum Doppler spread and sub-carrier spacing is approximately 33%. The equivalent baseband time-varying CIRs are generated following the method in VirTEX underwater acoustic channel simulator [13]. The CP-OFDM system setup is listed in Table I. The source bits are encoded by the convolutional code with the generator $[2335]_8$, and a random interleaver is applied. The total subcarriers are divided into $N_g = N/8$ groups. The pilot pattern for each group is $\left[0 \; P \; 0 \; D \; D \; D \; D \; D \right]$, where P and D represent pilot and data, respectively. Two scenarios are considered: (i) only pilot, (ii) pilot and data. In the former case, the receiver performs channel estimation by using only the received signal at pilot locations, while in the latter case both pilot and data locations are exploited with full knowledge of transmitted symbols assumed. These two cases represent the performance of an iterative receiver during the first and the last iteration. Moreover, the convergence of the iterative receiver is highly

TABLE I
CP-OFDM System Setting

Modulation	16QAM
Number of Subcarriers	1024
Symbol Rate	2 ks/s
CP Duration	50 ms
Carrier Frequency	12 KHz
Sampling Frequency	48 KHz

dependent on the performance of the first iteration and the performance in case (ii) can be regarded as the upper-bound of the iterative receiver. The raised cosine pulse with roll-off factor $\alpha = 1$ is used as pulse shaping filter and oversampling factor $G = 2$ is employed in simulations.

At the receiver side, the Bahl-Cocke-Jelinek-Raviv algorithm [14] is utilized for decoding. Also, CFO compensation is implemented by using the approach in [1]. The 2-D dictionary for DRM based channel estimator is constructed using $\Delta a = 1e-5$, $\lambda = 2$ in the oversampled case and $\Delta a = 1e-5$, $\lambda = 1$ in the symbol-rate sampled case. The iteration number for the OMP channel estimator is set to $M = 36$ for the oversampled case and $M = 24$ for the symbol rate sampled case. The parameters are chosen heuristically, while M in oversampled system should be larger than the symbol rate sampled receiver since the oversampled receiver has a finer grid to search. For the DPS based channel estimator, the maximum Doppler-spread frequency is chosen to be $f_{D_{max}} = 0.3$ Hz and the DPS-BEM model order is selected to be 3. Simulations with larger Doppler-spread frequency and higher model order have been run, showing performance degradation due to the channel estimation problem becomes highly underdetermined. The iteration number in the OMP algorithm is selected as $M = 18$ for the oversampled case and $M = 12$ for the symbol rate sampled case. The simulation is focused on investigating the impacts of oversampling on system performance.

Fig.1 shows the normalized mean square error (NMSE) performance of the channel estimator, defined as

$$\varepsilon_h = \frac{\mathrm{E}\left\{ |h(n,l) - \hat{h}(n,l)|^2 \right\}}{\mathrm{E}\left\{ |h(n,l)|^2 \right\}} \tag{22}$$

In the view of NMSE, the difference between the oversampled receiver and the symbol rate sampled receiver is small for DRM based receiver when only pilots are used for channel

This article has been accepted for publication in a future issue of this journal, but has not been fully edited. Content may change prior to final publication. Citation information: DOI 10.1109/LCOMM.2015.2423676, IEEE Communications Letters

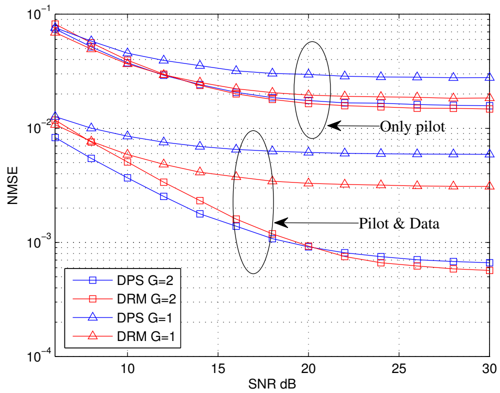

Fig. 1. NMSE performance for channel estimation

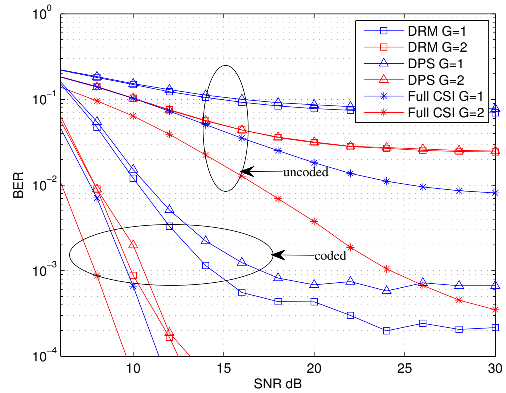

Fig. 2. BER performance of CP-OFDM system

estimation. In the DPS-BEM based receiver, the oversampled receiver achieves lower NMSE than the symbol rate sampled receiver. As for scenario (ii), the gain of the oversampled receiver over the symbol rate sampled receiver with respect to NMSE is increased.

Fig.2 shows the BER performance for both the symbol rate sampled receiver and the oversampled receiver. Performance in the case of perfect CSI available at the receiver (including knowledge of the noise variance) is presented as benchmark for comparison. In scenario (i), as for the uncoded BER performance, the oversampled receiver achieves significant gain over the symbol rate sampled receiver. The BER for the oversampled receiver decreases more quickly than the symbol rate sampled receiver. The oversampled receiver also has a much lower error floor, as a result of inter carrier interference, as compared to the symbol rate sampled receiver. As for the coded BER performance, the oversampled receiver achieves a gain around 5 dB at the BER level of 10^{-3}. Moreover, the oversampled receiver tends to achieve a much lower error floor than the symbol rate sampled receiver in the coded system. The BER for the coded oversampled receiver is below 10^{-4} when SNR is higher than 14 dB, while the BER for the coded symbol rate receiver is still above 10^{-4} when SNR is at 30 dB. It is also shown that the oversampled receiver achieves better performance than the symbol rate sampled receiver. Besides, the performance loss from the perfect CSI case is negligible in the case of coded systems while more significant in the case of uncoded systems. In simulation, the DRM achieves better performance than DPS in the coded system. But a deeper analysis between the two models requires extensive comparison under various system settings and experiments in real sea environment, and is out of the scope of this letter.

V. Conclusion

A time-domain oversampled OFDM system for communication over doubly-selective underwater acoustic channel is investigated. Two channel estimation methods, based on two widely-used time-varying channel models (i.e. DPS-BEM and DRM), are extended for oversampled OFDM system. The sparse channel estimation algorithm OMP is implemented. The performance of time domain oversampled CP-OFDM is verified through numerical simulations. Both the NMSE of the channel estimator and the system BER performance are presented. The BER performance shows that the oversampled receiver could achieve better performance in both coded situation and uncoded situation. In the coded CP-OFDM, the oversampled receiver obtains around 5 dB gain over the symbol rate receiver at the BER level of 10^{-3}.

References

[1] B. Li, S. Zhou, M. Stojanovic, L. Freitag, and P. Willett, "Multicarrier communication over underwater acoustic channels with nonuniform doppler shifts," *IEEE J. Ocean. Eng.*, vol. 33, no. 2, pp. 198–209, April 2008.

[2] C. Berger, S. Zhou, J. Preisig, and P. Willett, "Sparse channel estimation for multicarrier underwater acoustic communication: From subspace methods to compressed sensing," *IEEE Trans. Signal Process.*, vol. 58, no. 3, pp. 1708–1721, March 2010.

[3] Z. Chen, J. Wang, C. Zhang, and J. Song, "Time-domain oversampled receiver for OFDM in underwater acoustic communication," in *IEEE Veh. Tech. Conf. (VTC Fall)*, Sept 2014, pp. 1–5.

[4] Z. Wang, S. Zhou, G. Giannakis, C. Berger, and J. Huang, "Frequency-domain oversampling for zero-padded OFDM in underwater acoustic communications," *IEEE J. Ocean. Eng.*, vol. 37, no. 1, pp. 14–24, Jan 2012.

[5] J. Tao, J. Wu, Y. Zheng, and C. Xiao, "Oversampled OFDM detector for MIMO underwater acoustic communications," in *OCEANS 2010*, Sept 2010, pp. 1–5.

[6] J. Proakis, *Digital Communications*. McGraw-Hill, 2001.

[7] C. Tepedelenlioglu and R. Challagulla, "Low-complexity multipath diversity through fractional sampling in OFDM," *IEEE Trans. Signal Process.*, vol. 52, no. 11, pp. 3104–3116, Nov 2004.

[8] J. Wu and Y. Zheng, "Oversampled orthogonal frequency division multiplexing in doubly selective fading channels," *IEEE Trans. Commun.*, vol. 59, no. 3, pp. 815–822, March 2011.

[9] Z. Tang, R. Cannizzaro, G. Leus, and P. Banelli, "Pilot-assisted time-varying channel estimation for OFDM systems," *IEEE Trans. Signal Process.*, vol. 55, no. 5, pp. 2226–2238, May 2007.

[10] T. Zemen and C. Mecklenbrauker, "Time-variant channel estimation using discrete prolate spheroidal sequences," *IEEE Trans. Signal Process.*, vol. 53, no. 9, pp. 3597–3607, Sept 2005.

[11] P. Salvo Rossi and R. Muller, "Slepian-based two-dimensional estimation of time-frequency variant MIMO-OFDM channels," *IEEE Signal Process. Lett.*, vol. 15, pp. 21–24, 2008.

[12] T. Cai and L. Wang, "Orthogonal matching pursuit for sparse signal recovery with noise," *IEEE Trans. Inf. Theory*, vol. 57, no. 7, pp. 4680–4688, July 2011.

[13] J. Peterson and M. Porter, "Ray/beam tracing for modeling the effects of ocean and platform dynamics," *IEEE J. Ocean. Eng.*, vol. 38, no. 4, pp. 655–665, Oct 2013.

[14] L. Bahl, J. Cocke, F. Jelinek, and J. Raviv, "Optimal decoding of linear codes for minimizing symbol error rate (corresp.)," *IEEE Trans. Inf. Theory*, vol. 20, no. 2, pp. 284–287, Mar 1974.